Available online at www.sciencedirect.com

ScienceDirect

Procedia CIRP 58 (2017) 475 – 480

www.elsevier.com/locate/procedia

16th CIRP Conference on Modelling of Machining Operations

Machining simulation of Ti6Al4V under dry and cryogenic conditions

Stano Imbrogno[a,*], Stefano Sartori[b], Alberto Bordin[b], Stefania Bruschi[b], Domenico Umbrello[a]

[a]*Department of Mechanical, Energy and Management Engineering, University of Calabria, 87036, Rende (CS), Italy*
[b]*Department of Industrial Engineering, University of Padova, Via Venezia 1, 35131, Padova, Italy*

* Corresponding author. Tel.: +39 0984494637; fax: +39 0984494673. *E-mail address:* stano.imbrogno@unical.it

Abstract

Nowadays, numerical modeling is becoming a valuable and powerful tool for designing and optimizing the production process, as well as improving the machined components quality. Particularly, the Finite Element Method permits to increase the knowledge on the machinability of difficult-to-cut metals, such as the titanium alloys. The aim of this work is to develop a 3D FE model as a tool for predicting cutting forces, temperature, and machining-induced microstructural alterations during semi-finishing turning Ti6Al4V under dry and cryogenic conditions. The numerical model is experimentally calibrated and validated.

Keywords: Machining, Ti6Al4V, Finite Element Modeling, Cryogenic

1. Introduction

Among the titanium alloys, one of the most used is the Ti alloy grade 5, Ti6Al4V, due to its excellent combination of strength and toughness along with an excellent corrosion resistance. If, on one hand, its thermo-mechanical and chemical properties are preferred by the biomedical and aerospace industries, on the other hand, the alloying tendency and chemical reactivity, the low thermal conductivity and high strength at high temperature affect its machinability [1, 2]. Different techniques have been developed to improve the performances of manufacturing processes base on machining operations. In detail, the development of new cutting tool materials and tool design, the choice of the cutting parameters with respect of the employed cutting tools, and the application of advanced cooling techniques (e.g. compressed air jet, minimum quantity of lubricant and cryogenic fluids) have been successfully carried out [3,4]. Furthermore, the numerical models based on the Finite Element Method (FEM) help the designer to design and optimize the production process in order to understand the best operative parameters and avoid expensive experimental campaigns. Despite the power consumption, thermal field, tool wear, surface integrity, and overall quality of the product can be well predicted by numerical modeling [5], the overall simulation of the machining operations, namely turning, milling, drilling etc., still represents a challenge due to the computational complexity of the studied problem. In particular, several efforts for developing robust cutting simulation models based on 2D approach have been developed [7,8]. Calamaz et al. [8] and Özel et al. [7] developed new material behavior models able to take into account the plastic instability when the Ti6Al4V was machined; they implemented the new material flow stress models into FE softwares to predict the main variables such as cutting forces and temperature developed during the cutting process. However, the obtained results were based on a 2D approach under dry machining conditions, whereas very little information can be found about the implementation of these material models for simulating turning operations under cryogenic cooling conditions. Therefore, the aim of this work is to develop a 3D FE based model of turning operation for predicting the main fundamental variables of industrial interest, such as cutting forces, temperatures and affected layer thickness,

doi:10.1016/j.procir.2017.03.263

when a Ti6Al4V titanium alloy is machined under dry and cryogenic cooling conditions.

2. Experimental Procedure

2.1. Material and machining tests

The machined material under dry and cryogenic cooling conditions was the grade 5 titanium alloy Ti6Al4V supplied in bars. The metallographic analysis of the as-received material revealed an equiaxed microstructure in which the white areas were the α phase while the dark ones the β phase (Fig. 1).

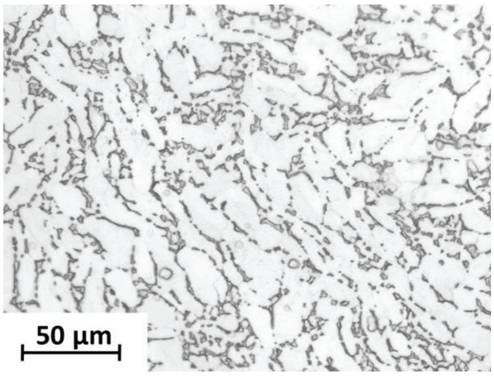

Fig. 1. Microstructure of Ti6Al4V alloy in the as-received condition.

The turning tests were conducted on a Mori Seiki NL 1500 CNC lathe, equipped with a system aimed at supplying the Liquid Nitrogen (LN_2) directly to the cutting zone. The LN_2 is carried through a vacuum insulated pipe (pressure 12 bar) and a nozzles system composed by two cooper nozzles with an internal diameter of 0.9 mm that direct the flow towards the tool rake face and the primary cutting edge with an inclination of 45°. The utilized cutting tool inserts were uncoated tungsten carbide tools, Sandvik Coromant® CNMG 120404 H13A, mounted on a PCLNR/L 2020k12 tool holder supplied by the same manufacturer. The effective cutting angles and the tools geometry were measured with a Sensofar Plu-Neox™ optical profiler by scanning the tool insert mounted on the tool holder. The effective cutting angles resulted of being equal to 7° and 8° for the rake and clearance angles respectively, while an approaching angle of 95° is defined by the tool holder geometry. The experimental set up as well as images of the turning tests are reported in Fig. 2. To measure the cutting forces and the thermal gradient, a Kistler®- type 9257 B three components piezoelectric dynamometer and an infrared camera FLIR A6000-series were employed respectively. A fresh cutting edge was adopted for each cryogenic and dry turning test, thus neglecting the tool wear effect in such short turning lengths. The turning trials were performed setting three cutting speeds (V_c), namely 70, 110 and 150 m/min, while the feed rate (f) and the Depth of Cut (DoC) were kept constant and equal to 0.2 mm/rev and 0.2 mm, respectively. The turning length was set in order to ensure a minimum cutting time of 30 seconds to reach the steady state conditions for the cutting force and temperatures. After the turning tests, samples were collected from the machined bars, embedded into a phenolic resin, ground, polished and etched for metallographic analysis in order to estimate the machined affected layer. The measurements were carried out by using a FEI QUANTA 450™ SEM equipped with the BSED probe, for each samples the analysis was conducted in three different points of the machined surfaces. The experimental outcomes were used in the numerical calibration step for estimating the friction coefficients and for validating the developed FE model.

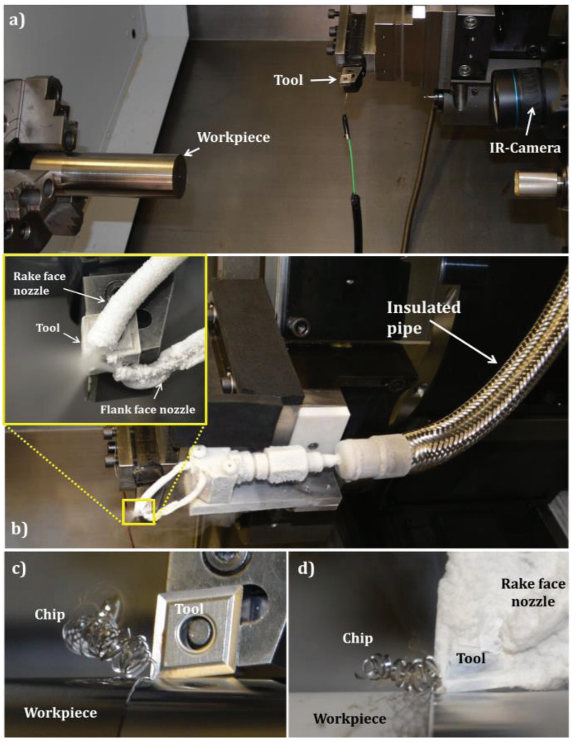

Fig. 2. a) Experimental set-up; b) cryogenic delivery set-up; c) V_c=10m/min, f=0.2mm/rev dry machining; d) V_c=110m/min, f=0.2mm/rev cryogenic machining.

3. Numerical procedure

3.1. Modelling of the material behavior

Most of the material constitutive models for simulating the thermo-mechanical behavior of the wrought Ti6Al4V are based on the renowned Johnson-Cook (JC) flow stress law [9-11]. The titanium alloys, in particular the Ti6Al4V, exhibit different behavior depending on the strain and temperature. Molinari et al. [12] observed the formation of Adiabatic Shear Bands (ASB) into the chips, as a demonstration of the thermo-mechanical instability resulting in the concentration of large shear deformations in narrow layers. Other researchers observed the formation of ASB in several cutting tests even at low cutting speed [12-13].

In detail, Calamaz et al. [8] proposed a new material model to take into account not only the strain rate hardening and the thermal softening phenomenon, but also the strain softening phenomenon that characterizes the Ti6Al4V under severe plastic deformation conditions. The main feature of the new mathematical formulation named TANH (Hyperbolic TANgent) is to add a new term to the JC law in order to model the strain softening effect. The material behavior model implemented via sub-routine is represented by Eq. 1.

$$\sigma = \left(A + B\varepsilon^n\left(\frac{1}{\exp(\varepsilon^a)}\right)\right)\left(1 + C\,ln\left(\frac{\dot{\varepsilon}}{\dot{\varepsilon}_0}\right)\right)\left(1 - \left(\frac{T - T_r}{T_m - T_r}\right)^m\right) \times$$
$$\times\left(D + (1 - D)\,tanh\left(\frac{1}{(\varepsilon + S)^c}\right)\right) \quad (1)$$

Where:

$$D = 1 - \left(\frac{T}{T_m}\right)^d \text{ and } S = \left(\frac{T}{T_m}\right)^b$$

The coefficients A, B, C, n and m are reported in [14] while the other constants in [7]. The σ is the flow stress, ε the true strain, $\dot{\varepsilon}$ the true strain-rate, T_r and T_m are the room temperature and work material melting, respectively.

3.2. FE Model

The commercial FEA code SFTC Deform 3D® was utilized to simulate the turning operations. The cutting tool was modeled as a rigid body (divided into 58000 elements) and a mesh window was set on the cutting edge in order to better approximate the radius of the edge. The workpiece was modeled as an isotropic hardening material, which was divided into 150000 elements. Regarding the mesh density on the workpiece, the elements in the cutting zone and along the machined surface were fifty times as dense as the other ones that presented a length of 10 µm (Fig. 3a). The choice of very small elements also allowed to better predict the extension of the plastic deformation area below the machined surface.

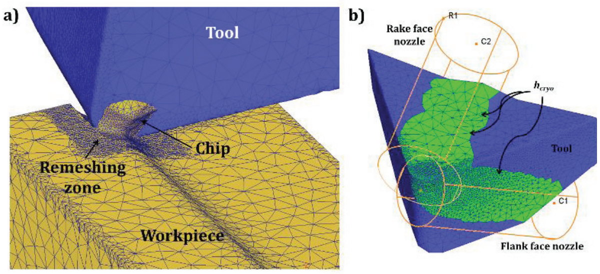

Fig. 3. a) 3D FE model; b) Modeling of cryogenic environment on rake and flank face.

Moreover, aiming at achiving an accurate prediction of the process variables (strain, temperature within the machined surface layers), a dynamic local remeshing window (remeshing zone) was set following the tool. The adopted remeshing strategy permits to avoid a wrong prediction of the deformed zone because of the interpolation of the data with the coarse mesh (few microns below the machined surface) and preserves the right values of the fine mesh since the global remeshing does not occur. The latter is an important characteristic of the FE model since few microns of plastically deformed layers have to be predicted. The workpiece was fixed, therefore no movements were allowed while the tool was able to move along the cutting direction. Both the parts were set to exchang heat with the environment, by setting a convection coefficient equal to 20 W/(m^{2}K), which is the standard value for free-air convection. In order to simulate the presence of the cryogenic fluid, its thermal effect on the heat exchange was taken into account. The cryogenic cooling effect was modeled by setting three local windows: the first one was set into the chip-tool interface, the other two were oriented taking into account the position of the nozzles on the tool (Fig 3b). The local temperature inside these windows was set equal to -196 °C while the convection coefficient, namely h_{cryo}, was computed as reported in [15]. Aiming at reaching a thermal steady state condition at the tool-chip interface in a short computational time, with the assumption of a thermally perfect contact, a global heat transfer, h_{int}, was set equal to 100000 kW/(m^{2}K), according to the literature results [5,6]. Finally, a sticking-sliding friction model (sticking governed by the shear model $\tau = m\tau_0$; sliding governed by the Coulomb model $\tau = \mu\sigma$) was also implemented. The friction coefficients m and µ were calibrated using the outcomes of tests under dry and cryogenic cooling conditions.

3.3. FE calibration

The aim of the calibration phase was to identify the friction coefficients, namely m and μ, of the sticking-sliding friction model. At the beginning of the calibration procedure, two initial values were set and then modified as suggested by the routine reported in Fig. 4.

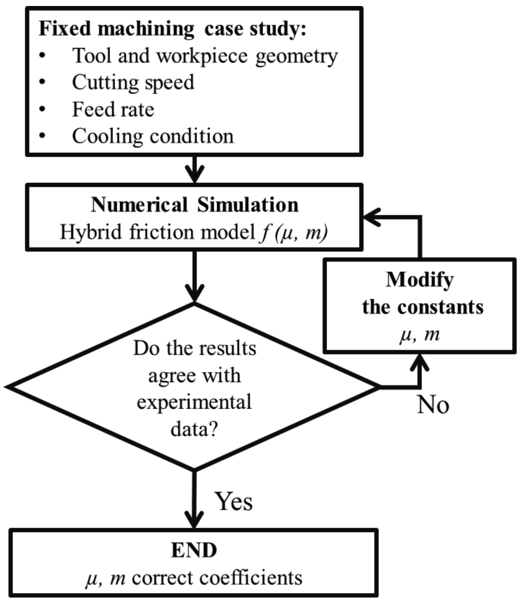

Fig. 4. Calibration procedure for the friction coefficients.

The procedure was used for the machining simulation under both dry and cryogenic cooling conditions setting a cutting speed of 70 m/min, feed rate of 0.2 mm/rev and DoC of 0.2 mm.

Once the cumulative percentage error evaluated comparing the predicted cutting forces and temperature with the experimental outcomes reached a value lower than 5%, the procedure was stopped and the friction coefficients were then determined and used in the model.

4. FE Validation, results and discussions

Through the calibration phase it was possible to define the right value of the friction coefficients. The calibrated constants of the hybrid friction model for dry and cryogenic conditions are reported in Table 1

Table 1. Calibrated friction coefficients depending on the cooling conditions.

Cooling condition	m	μ
Dry	0.95	0.8
Cryogenic	0.6	0.5

As reported in Table 1, the values obtained from machining under dry conditions are higher than the ones calibrated when LN_2 is delivered. These numerical results are in agreement with the experimental evidences reported in [16, 17]. Indeed, the liquid nitrogen. (liquid phase) delivered into the cutting zone has a positive effect in terms of reduction of thermal gradient and reduction of cutting forces due to the combination of lubrication and embrittlement effects. Subsequently, the validation phase was applied to simulate the other investigated cases. All the numerical results, in terms of Main Cutting Force (F_c), Feed Force (F_f) and Temperature, were collected and compared with the experimental ones. As shown in Figs. 5, 6 and 8, the developed FE model is able to correctly predict the trend and the numerical values of the experimental outcomes.

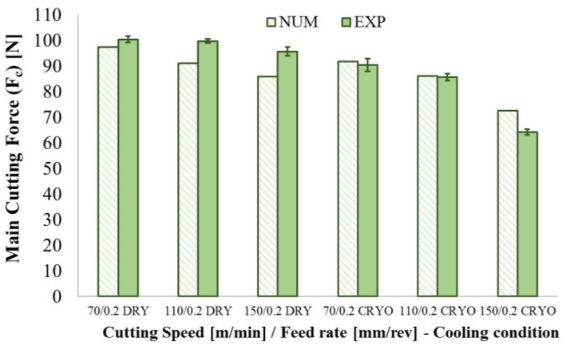

Fig. 5. Comparison between the numerical and experimental Main Cutting Force (Fc).

Indeed, at increasing the cutting speed, the F_c and F_f decrease due to the increment of the temperature (thermal softening effect) and this thermo-mechanical response is well represented by the model. In detail, by comparing the predicted data with the experimental ones in dry and cryogenic cooling conditions, the average error is less than 8% and 7% in predicting the F_c and 18% and 12% in predicting the F_f, respectively.

Figure 7 shows a comparison between the predicted and evaluated temperature during the turning process under cryogenic conditions. For measuring the thermal gradient, the cutting zone (where chip is continuously forming) was taken into account as reported in Fig. 7b. Once the temperature reached the steady state, the data were collected and the average value was computed for each cutting test. The same procedures were employed with the results predicted by the FE simulation and the same position of the cutting zone considered in Fig. 7b was considered in the numerical simulation as shown in Fig. 7a.

The temperature predicted by the model are in good agreement with the ones observed during the turning tests. Moreover, the FE model slightly overestimates the thermal gradient in dry conditions and underestimates (except the case with cutting speed of 70 m/min) the thermal gradient in cryogenic conditions.

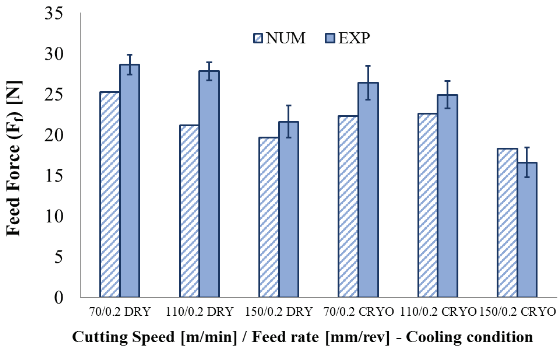

Fig. 6. Comparison between the numerical and experimental Feed Force (Fc).

These results can justify the underestimation and overestimation of the F_c in dry and cryogenic conditions respectively, because the variation of the thermal gradient governs the competition between the thermal softening and strain hardening. Generally, the average error in the temperature prediction is between the 1% and 6%.

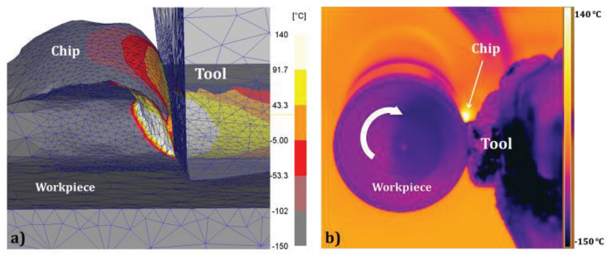

Fig. 7. a) Predicted temperature in the cutting zone; b) temperature acquired via IR camera (V_c=70m/min, f=0.2mm/rev cryogenic conditions).

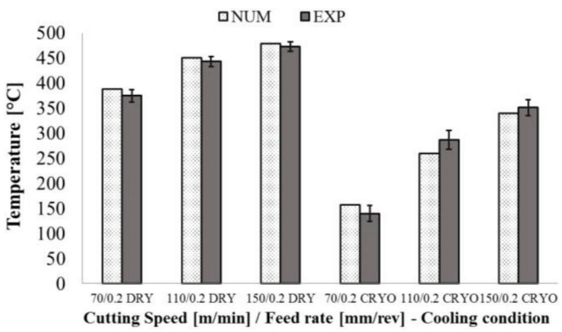

Fig. 8. Comparison between the numerical and experimental temperature.

Furthermore, the good prediction of the temperature when using cryogenic fluid confirms the validity of the implemented convective heat transfer model. To investigate the metallurgical alterations that usually occur during machining operation, a Scanning Electron Microscope (SEM) analysis was carried out on the cross section of the machined bars. The cutting parameters and the tool used during the tests as well as the cooling strategy did not affect the machined materials. Indeed, no metallurgical phenomena (e.g. dynamic recrystallization, white layers formation) were detected, therefore no grain size predictive model was implemented into sub-routines.
Finally, a comparison between the affected layer estimated by SEM analysis and the plastic deformed layer predicted by the simulation was carried out. Fig. 9a represents the cross section of a machined sample and the numerical prediction of the effective strain (Fig. 9b). The thickness of the material subjected to high plastic strain behind the simulated machined surface was compared with the experimental one observed via SEM: the predicted layer of the plastic strain is very similar with the one of Fig. 9a in which the grains appear strongly deformed and elongated along the cutting direction.

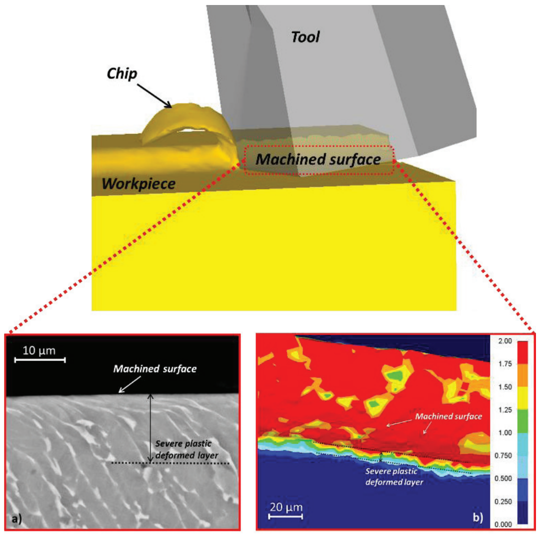

Fig. 9. a) SEM micrograph of the machined sample (V_c 110m/min, dry conditions); b) effective plastic strain (mm/mm) predicted by FE model.

Regardless of the cooling strategies and tested cutting parameters the experimental measurements highlighted that the deformed layer values are between 8.5 and 10.4 µm, values comparable with those obtained through the numerical model which respectively vary between 9 to 10 µm.

5. Conclusions

This work presents a 3D FE based model of a turning operation carried out on a titanium alloy (Ti6Al4V) under dry and cryogenic cooling conditions. Although many flow stress models were developed for modeling the mechanical behavior of Ti6Al4V, the one proposed by Calamaz et al. [8] provided the best results in terms of cutting forces and temperatures. The TANH hyperbolic model permits to take into account the strain-thermal softening effect that characterizes this alloy under different strain, strain-rate and temperature conditions depending on the cooling strategy. The mechanical behavior model coupled with a hybrid friction model based on sticking-sliding effect was implemented via sub-routine and calibrated for the two different cooling conditions. The friction coefficients calibrated under cryogenic conditions are lower than the ones obtained in dry conditions highlighting the benefit of the LN_2 delivered during the turning process (lower temperature and cutting forces). As reported from the experimental results, the increasing of the cutting speed provokes a decreasing of the cutting forces due to the thermal-softening behavior but an increasing of the thermal gradient into the cutting zone: these trends and results are well numerically predicted by the developed model. A SEM analysis for investigating the surface and sub-surface conditions after machining was also carried out. No metallurgical phenomena, such as dynamic recrystallization, white layer formations, were found but only strongly deformed grains within the affected layer. The thickness of the deformed layer observed via SEM analysis was compared with the effective plastic strain thickness predicted by the FE model. The numerical predictions are in good agreement with the experimental observation. This latter lays the foundation for future works in which a development of physics model for taking into account strain hardening rate due to the deformation of the material is the key for better understanding the surface integrity of the products.

References

[1] Donachie M. J., Titanium: A Technical Guide, 2nd Edition. ASM International; 2000.
[2] Lütjering G., Williams Donachie J. C., Titanium, 2nd Edition. Springer; 2007.
[3] Davim J.P., Machining of Titanium Alloys, edited by J.P Davim, Springer 2014
[4] Rotella G., O. Dillon Jr W., Umbrello D., Settineri L., Jawahir I. S., The effects of cooling conditions on surface integrity in machining of Ti6Al4V alloy, Int J Adv Manuf Technol, 2014, 71: 47-55.
[5] P.J. Arrazola, T. Özel, D. Umbrello, M. Davies, I.S. Jawahir (2013), Recent advances in modelling of metal machining processes, CIRP Annals-Manufacturing Technology 62:695–718.
[6] J. P. Davim, Machining of Hard Material, Springer 2010, 150-172.
[7] Sima M, Özel T., Modified material constitutive models for serrated chip formation simulations and experimental validation in machining of

titanium alloy Ti–6Al–4V. International Journal of Machine Tools and Manufacture 50 (11) (2010) 943-960.
[8] Calamaz M., Coupard D., Girot F. A., A New Material Model for 2D Numerical Simulation of Serrated Chip Formation When Machining Titanium Alloy Ti–6Al–4 V, International Journal of Machine Tools and Manufacture 48(3-4) (2008):275-288
[9] Johnson G.-R., Cook W.-H., A constitutive model for metals subjected to large strains, high strain rates and high temperatures, in: Proceedings of the Seventh International Symposium on Ballistics, Hague, Netherlands, vol. 54,1983, pp. 1–7.
[10] Shrot A., Bäker M., Determination of Johnson–Cook parameters from machining simulations. Computational Materials Science 52 (1) (2012) 298-304.
[11] Umbrello D., M'Saoubi R., Outeiro J.C., The influence of Johnson–Cook material constants on finite element simulation of machining of AISI 316L steel. International Journal of Machine Tools and Manufacture 47 (3–4) (2007) 462-470.
[12] Molinari A., Musquar C., Sutter G., Adiabatic shear banding in high speed machining of Ti–6Al–4V: experiments and modeling, International Journal of Plasticity 18 (2002) 443–459.
[13] Ye G.G., Xue S.F., Jiang M.Q., Tong X.H., Dai L.H., Modeling periodic adiabatic shear band evolution during high speed machining Ti-6Al-4V alloy, International Journal of Plasticity 40 (2013) 39–55.
[14] Lee W.S., Lin C.F., Plastic deformation and fracture behavior of Ti–6Al–4V alloy, Materials Science and Engineering A 241 (1998) 48–59.
[15] Umbrello D., Caruso S., Imbrogno S. (2016) Finite element modelling of microstructural changes in dry and cryogenic machining AISI 52100 steel, Materials Science and Technology, 32:11, 1062-1070
[16] Shane Y. Hong , Yucheng Ding & Jason Jeong (2002) Experimental evaluation of friction coefficients and liquid nitrogen lubrication effect in cryogenic machining, Machining Science and Technology, 6:2, 235-250,
[17] Courbon C., Pusavec F., Dumont F., Rech J., Kopac J., Tribological behaviour of Ti6Al4V and Inconel718 under dry and cryogenic conditions—Application to the context of machining with carbide tools, Tribology International 66 (2013) 72–82.